Environ Monit Assess (2017) 189: 582
https://doi.org/10.1007/s10661-017-6281-z

Relationships of relative humidity with $PM_{2.5}$ and PM_{10} in the Yangtze River Delta, China

Cairong Lou · Hongyu Liu · Yufeng Li · Yan Peng · Juan Wang · Lingjun Dai

Received: 15 April 2017 / Accepted: 5 October 2017 / Published online: 23 October 2017

Abstract Severe particulate matter (PM, including $PM_{2.5}$ and PM_{10}) pollution frequently impacts many cities in the Yangtze River Delta (YRD) in China, which has aroused growing concern. In this study, we examined the associations between relative humidity (RH) and PM pollution using the equal step-size statistical method. Our results revealed that RH had an inverted U-shaped relationship with $PM_{2.5}$ concentrations (peaking at RH = 45–70%), and an inverted V-shaped relationship (peaking at RH = 40 ± 5%) with PM_{10}, SO_2, and NO_2. The trends of polluted-day number significantly changed at RH = 70%. The very-dry (RH < 45%), dry (RH = 45–60%) and low-humidity (RH = 60–70%) conditions positively affected $PM_{2.5}$ and exerted an accumulation effect, while the mid-humidity (RH = 70–80%), high-humidity (RH = 80–90%), and extreme-humidity (RH = 90–100%) conditions played a significant role in reducing particle concentrations. For PM_{10}, the accumulation and reduction effects of RH were split at RH = 45%. Moreover, an upward slope in the $PM_{2.5}/PM_{10}$ ratio indicated that the accumulation effects from increasing RH were more intense on $PM_{2.5}$ than on PM_{10}, while the opposite was noticed for the reduction effects. Secondary transformations from SO_2 and NO_2 to sulfate and nitrate were mainly responsible for $PM_{2.5}$ pollution, and thus, controlling these precursors is effective in mitigating the PM pollution in the YRD, especially during winter. The conclusions in this study will be helpful for regional air-quality management.

Keywords Relative humidity (RH) · Association · Particulate matter · Equal step-size statistical method

Yufeng Li, Yan Peng, Juan Wang, and Lingjun Dai are co-authors.

C. Lou · H. Liu (✉) · Y. Li · J. Wang · L. Dai
Key Laboratory of Virtual Geographic Environment, Nanjing Normal University, Ministry of Education, Nanjing, Jiangsu 210023, China
e-mail: liuhongyu@njnu.edu.cn
C. Lou
e-mail: loucairong@126.com

Y. Li
e-mail: pandale_0826@163.com

J. Wang
e-mail: wangjjsyctu@163.com

L. Dai
e-mail: dailinjun@hotmail.com

C. Lou
College of Geographic Sciences, Nantong University, Nantong 226007, China

C. Lou · H. Liu · Y. Li · J. Wang · L. Dai
State Key Laboratory Cultivation Base of Geographical Environment Evolution (Jiangsu Province), Jiangsu Center for Collaborative Innovation in Geographical Information Resource Development and Application, College of Geographical Science, Nanjing Normal University, Nanjing 210023, China

Y. Peng
Nantong Meteorological Bureau, Nantong 226007, China
e-mail: pengxiaoyan208@163.com

Introduction

Severe haze pollution caused by $PM_{2.5}$ and PM_{10} (PM) has attracted great concern worldwide due to the impairment effects on climate, living environment, and particularly human health (Naeher et al. 1999; Pui et al. 2014; Gao et al. 2015). According to the data released by the Chinese Ministry of Environmental Protection (CMEP) in 2015, 78.4% of the prefecture-level cities in China suffered severe PM pollution (CMEP 2016), most of which are located in three Chinese developed regions, the Jing-Jin-Ji Delta, the Yangtze River Delta (YRD), and the Pearl River Delta (Han et al. 2014; Hu et al. 2014). Furthermore, in 2014, dust-suppressing vehicles equipped with fog guns were used to remove particles in the air by spraying water into the air (http://news.mydrivers.com/1/313/313236.htm) in several Chinese cities (such as Xi'an and Shijiazhuang), which aroused public attention and sparked an intense controversy in the scientific community. There is an urgent need to explore the drivers of PM to mitigate the regional air pollution in China today.

Recent studies have suggested that conventional meteorological conditions, such as wind speed (WS), temperature (T), and precipitation, have distinct effects on $PM_{2.5}$ and PM_{10} concentrations besides anthropogenic emissions (Tran and Molders 2011; Kassomenos et al. 2014; Wang and Ogawa 2015). For example, low WS, low T, and a strong temperature inversion may cause PM concentration to increase (Tran and Molders 2011; Hsu and Cheng 2016), while increased precipitation can scavenge particles from the air (Tai et al. 2010; Przybysz et al. 2014; Ouyang et al. 2015). However, there are large gaps in understanding correlations between relative humidity (RH) and PM pollution, partly due to the uncertainty about PM sensitivity to RH and to their nonlinear relationship (Wang et al. 2014; Wang et al. 2015). PM is a complex mixture of primary particles (directly emitted from anthropogenic activities) and secondary particles, which are formed by reactions of the precursors (i.e., SO_2 and NO_2) (Stone et al. 2010; Huang et al. 2011; Hasheminassab et al. 2014; Cheng et al. 2015). Many of the present study's conclusions suggest that RH significantly influences PM from its formation to dispersion through both physical and chemical processes, such as affecting the rates of deliquescence, gas-to-particle conversion, hygroscopic growth, and wet or dry deposition (Wang et al. 2014; Cheng et al. 2015; Liu et al. 2016a, b).

Nevertheless, it is still unclear whether an increase in RH can reduce haze pollution or not. On the one hand, some articles indicated that an increase in RH was conducive to particle deposition. For instance, studies of wetlands suggest that strong evaporation and transpiration in the presence of water or wetlands could form a microclimate with lower temperature and higher RH compared with the surrounding environment (Sun et al. 2012; Anda et al. 2015; Du et al. 2016), which may decrease the gas-to-particle conversion rate and favor particle deposition (Catinon et al. 2012; Kang et al. 2015). On the other hand, positive correlations between RH and $PM_{2.5}$ were identified in studies conducted in Beijing (Cheng et al. 2015; Zhu et al. 2016), Shanghai (Xu et al. 2015), and the YRD (Hua et al. 2015), indicating that an increase in RH could aggravate PM pollution. Additionally, several authors have examined the influence of different RH levels on PM concentrations. Wu et al.(2016) explored the association between the size distribution of PM and RH in Nanjing and suggested that particle sizes changed significantly for RH = 70%, which was closely related to the hygroscopic growth of particles. Wang et al.(2014) divided RH into three stages: stage 1 (RH < 35%), characterized by a low secondary conversion rate (from SO_2 and NO_2 to sulfate and nitrate) and slow hygroscopic growth; stage 2 (RH = 35–50%), characterized by accelerated secondary conversion and an enhanced hygroscopic growth rate; and stage 3 (RH = 50–75%), characterized by an explosive increase in fine particles. For PM deposition, large-sized particles (e.g., PM_{10}) were easy to be deposited due to gravity, while the small-sized particles remained suspended in the air until they had accumulated sufficient mass through hygroscopic growth, aggregation, and merging with each other (Langner et al. 2011; D'Angelo et al. 2016). Moreover, particles can also be dissolved in rain, snow, or fog, all of which are characterized by extreme high RH, and then deposited on the ground along with the precipitation (Matsuda et al. 2010; Witkowska and Lewandowska 2016). Thus, RH is a very important factor that directly affects the transformation and feature of particles.

However, the present conclusions about specific impacts of RH on PM are still fragmented and ambiguous, and debates on whether or not to mitigate haze pollution via spraying water into the air are ongoing. Furthermore, studies regarding the relationships of RH with PM are relatively limited, and most of them are mainly focused spatially on the urban scale and temporally over a few

days or several decades. Considering that the effects of anthropogenic emissions (Hao and Liu 2016), surface terrain, and vegetation on PM (Tallis et al. 2011; Masiol et al. 2014; Salameh et al. 2015) may be much stronger than those of meteorological variables (particularly RH), it is necessary to minimize those disturbances as much as possible to accurately evaluate the correlations of RH with PM pollution. For these reasons, we selected the YRD as the sample area and focused entirely on the impacts of RH on $PM_{2.5}$ and PM_{10} concentrations in this study. The following aspects were considered. First, some studies have proposed that the frequent haze episodes in the YRD were potentially related to its high humid environment (Hua et al. 2015). Second, compared with the national scale, the climate in the YRD is more homogeneous and the synoptic conditions have the same variation patterns in every city (e.g., the occurrence of rainfall or extreme weather conditions). Similarly, the socioeconomic differences in the YRD are relatively small. Therefore, the impacts from the spatial differences of various factors on PM pollution can be reduced to some extent owing to the similar characteristics in sample cities. Additionally, these spatial differences can be further reduced by using the PM anomaly values (Wang et al. 2012). All the abovementioned considerations established the feasibility for this study. To the best of our knowledge, none of the previous studies have analyzed the association between RH and PM in the YRD.

In general, our goals in this paper are to characterize the variation patterns of $PM_{2.5}$ and PM_{10} in the YRD and further explore their relationships with RH. We will discuss (1) the spatiotemporal characteristics of $PM_{2.5}$ and PM_{10}, (2) the relationship of PM with RH and the seasonality, and (3) effects of other factors, such as temperature, and precursor concentrations (SO_2 and NO_2), on PM. This study will provide information regarding humidity impacts on haze pollution to the local government for optimizing an emergency environmental plan.

Materials and methods

Study area

The YRD located in the east of China (Fig.1 (a1)) is one of six influential metropolitan regions in the world and one of three developed areas in China, playing a very important role in Chinese socioeconomic development (Tian et al. 2011). The region is an alluvial plain formed before the Yangtze River enters the sea, and it has an average elevation of 2 m. Different boundaries of the YRD have been delimited for varied study purposes. In this study, considering the spatial distribution of PM monitoring sites and data availability, our study area in the YRD only includes 16 cities (Fig. 1 (a2, a3)). They are Shanghai, eight cities in Jiangsu province (i.e., Nanjing, Suzhou, Wuxi, Changzhou, Nantong, Zhenjiang, Taizhou(j), and Yangzhou), and seven cities in Zhejiang province (i.e., Hangzhou, Jiaxing, Huzhou, Shaoxing, Ningbo, Taizhou(z), and Zhoushan), respectively. This region covers 1.1% (about 110,800 km^2) of China in terms of area but accounts for 7.47% of the total population according to the statistical data of 16 cities in 2014.

Belonging to the subtropical monsoon climate zone, the region has a moderate climate and four distinctive seasons. In 2014–2015, the area has an annual average precipitation of 1000–2000 mm and an annual mean temperature of 17 °C. The YRD has the densest river network (4.8–6.7 km/km^2) in China, with an average water resource of 539.79 billion cubic meters (Fig. 1 (a3)). Pursuant to data from the National Science and Technology Infrastructure platform (http://nnu.geodata.cn), various wetlands in the YRD cover a total area of 13,000 km^2. All of these factors cause the region to have a high humidity environment, with an annual average RH of 75 ± 5%.

Data selection

In this paper, we mainly used two datasets: air-quality data (daily $PM_{2.5}$, PM_{10}, SO_2, and NO_2 concentrations) and meteorological data (daily RH, T, WS, WD, and precipitation values). In the YRD region, there are 121 national air-quality monitoring sites as shown in Fig. 1 (a3). Among them, 98 sites are located in prefecture-level cities (black dots) and 23 are located in county-level cities (gray dots). Air-quality data from these monitoring sites are updated on the air-quality publishing platform of the Chinese National Environmental Monitoring Centre at a temporal resolution of 1 h (http://datacenter.mep.gov.cn/index). Considering that most of air-quality monitoring sites are situated in urban built-up areas, we selected 98 urban sites and obtained their air-quality data for this paper, the aim being to reduce the diversity of PM concentrations and increase their comparability across the cities. Correspondingly,

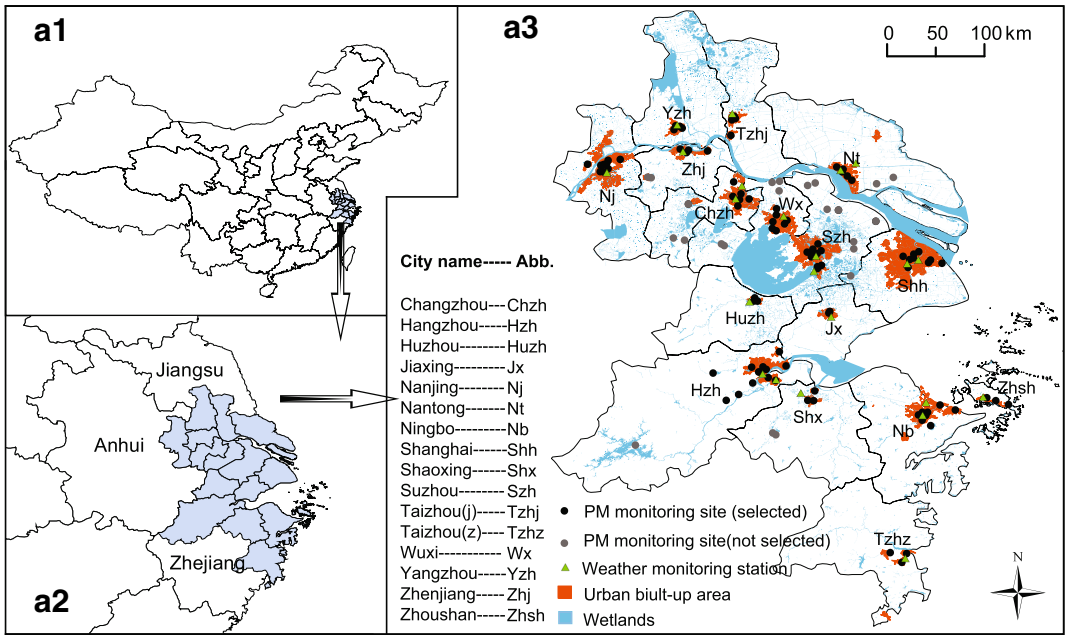

Fig. 1 Location of the YRD in China (a1, a2) and the spatial distribution of 120 air-quality monitoring sites and 22 meteorological stations in the YRD (a3)

22 weather monitoring sites located in urban built-up areas were carefully chosen to obtain their hourly meteorological data, which are updated on the website (http://www.cma.gov.cn/2011qxfw/2011qtqyb/) of the China Meteorological Administration, to match the PM data. These hourly raw values are collected from January 1, 2014, to December 31, 2015.

The raw data were preprocessed according to the requirements for measuring air pollutant concentrations in the Chinese average annual standard (GB 3095-2012) issued by the CMEP. We deleted the values less than 0 and the abnormal concentrations, and then calculated the daily concentration by averaging the 24-h values from 0:00 to 23:00. If the raw data were continuously missing for more than 4 h in a day, the relevant daily concentrations were considered invalid and excluded. Further, we computed a daily PM concentration of a certain city by averaging the corresponding daily PM concentrations of all monitoring sites for that city. The daily meteorological variables in a city were obtained in the same manner.

It should be noted that we used daily averages for all the variables to avoid statistical biasing related to their inherently diurnal changes. Additionally, we divided the 12 months of a year into four seasons: winter (December, January, and February), spring (March, April, and May), summer (July, June, and August), and autumn (September, October, and November). In our study, a polluted day was defined as a day with daily $\rho(PM_{2.5}) \geq 75\ \mu g/m^3$, and a clear day refers to the day with the daily $\rho(PM_{2.5}) < 75\ \mu g/m^3$. Based on the previous definition, a pollution episode was defined as a period of time with a clear day, followed by no less than two consecutive polluted days, followed by a clear day. That is, the duration of one pollution episode was at least 4 days long, following the sequence "one clear day + more than 2 polluted days + one clear day."

Methods

Equal step-size statistic method

An equal step-size statistical method was used to explore the association of RH to PM. For example, the relationship between RH and $PM_{2.5}$ based on the step-size = 5% was calculated and the specific process was listed as follows:

If step-size = 5%, RH (0–100%) will be equally divided into 20 ranges, such as RH_1 = 0–5%, RH_2 = 5–10%, …, RH_n = 5 $(n-1)$%–5n% (n = 1, 2, 3……20), and then the $PM_{2.5}$ concentration during the RH_n range can be approached by Eq. 1.

$$C_n = \frac{1}{m}\sum_{i=1}^{m} C_m \quad (1)$$

where m refers to the number of all $PM_{2.5}$ concentrations during the RH_n range, and each of them is written as C_m. C_n refers to the mean of all C_m. In our study, C_n was taken as the average $PM_{2.5}$ concentration of RH_n.

In this paper, we used three step-sizes (1, 2, and 5%) to explore the relationships of RH with $PM_{2.5}$, PM_{10}, SO_2, and NO_2 in our study. Although more specific information may be neglected at a larger step-size, the regularity of the curve is clearer. Moreover, due to the requirement of the linear regression model, we used the statistical results at the step-size of 1 or 2% to supply enough data for linear fitting.

Anomaly processing of data

To reduce the difference of air-quality data that are driven by the geographical background of monitoring sites and other influencing factors, we used the anomaly value of daily air-quality variables in our paper. Using $PM_{2.5}$ as an example, the formula was written as Eq. 2.

$$\Delta C_{d-PM2.5} = C_{d-PM2.5} - \overline{C}_{a-PM2.5} \quad (2)$$

where $\Delta C_{d-PM2.5}$ presents a daily anomaly concentration of $PM_{2.5}$ at a monitoring site, $C_{d-PM2.5}$ refers to its daily actual concentration, and $\overline{C}_{a-PM2.5}$ refers to the annual $PM_{2.5}$ concentration of this monitoring site. In the same way, PM_{10}, SO_2, and NO_2 concentrations were all used in the anomaly values.

Univariate linear regression

To express the response of PM to RH, we employed univariate linear regression to determinate the RH effects. The formula is written as Eq. 3.

$$y = a + bx \quad (3)$$

where y presents an air-quality index ($PM_{2.5}$, PM_{10}, SO_2, or NO_2); x means the RH value; a refers to the constant; and b stands for the slope of the regression line, which expresses the elasticity of y growth caused per unit of x added.

In the following text, we use a T test to evaluate the significance level of the relationships between RH and PM or the other pollution variables in SPSS 20.0 software, including univariate linear fitting and Pearson correlation analysis.

Results

Characteristics of PM pollution in the YRD

In 2014–2015, the YRD suffered serious haze pollution (Table 1) with the annual ρ($PM_{2.5}$) of 58 μg/m^3, which was 5.8 times higher than that of the World Health Organization standard (10 μg/m^3), and 1.7 times higher than that of the Chinese average annual standard (GB3095-2012) issued by the CMEP (35 μg/m^3). Compared with 2014, the PM pollution in 2015 had a slight reduction, with a drop of 7 μg/m^3 in annual ρ($PM_{2.5}$) and a decrease of 9 μg/m^3 in annual ρ(PM_{10}). Seasonal variations of $PM_{2.5}$ (Table 1 and Fig.1) are characterized by "highest in the winter (80μg/m^3), followed by in the spring (57μg/m^3) and in the autumn (49μg/m^3), and lowest in summer (44μg/m^3)." The seasonal trends of PM_{10} and pollution days tracked the patterns of $PM_{2.5}$. Almost 50% of pollution days occurred in the winter time.

Table 1 Statistics of annual and seasonal PM concentrations and total pollution days of the YRD in 2014–2015

	Mean $PM_{2.5}$ (μg/m^3)			Mean PM_{10} (μg/m^3)			$PM_{2.5}$ pollution days (days)		
	2014	2015	Annual mean	2014	2015	Annual mean	2014	2015	Total
Winter	78	81	80	113	119	116	39	42	81
Spring	63	50	57	103	84	94	26	13	39
Summer	49	38	44	74	63	68	15	4	19
Autumn	52	46	49	83	76	80	16	12	28
Year	61	54	58	94	85	89	96	71	167

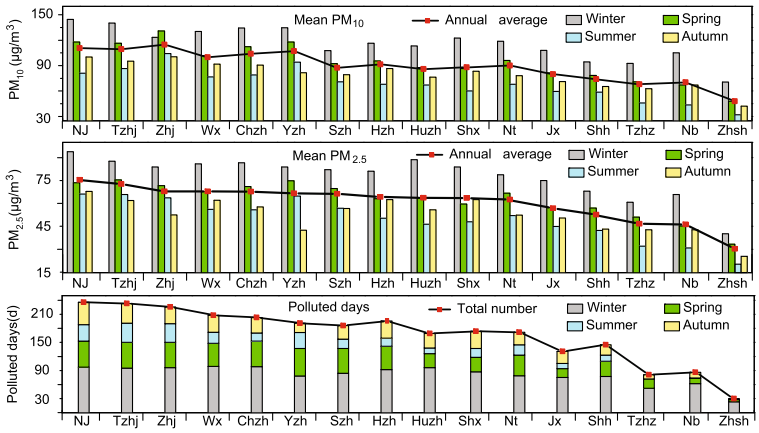

Fig. 2 Statistics of annual and seasonal $PM_{2.5}$ and PM_{10} concentrations and total polluted days of each city in the YRD

As illustrated in Fig. 2, 16 cities witnessed the annual $\rho(PM_{2.5})$ of 35–66 μg/m^3 and the annual $\rho(PM_{10})$ of 46–107 μg/m^3. Only one city, Zhoushan, had an annual $\rho(PM_{2.5})$ of less than 35 μg/m^3 and an annual $\rho(PM_{10})$ of 46 μg/m^3. The remaining cities all suffered severe haze pollution. Among them, the top five cities (including Nanjing, Taizhou(j), Zhenjiang, Wuxi, and Changzhou) had an annual $\rho(PM_{2.5})$ of more than 62 μg/m^3 and the total pollution days of 221 ± 17 days in 2 years. Moreover, 50% of the sample cities in this region experienced more than 180 pollution days in 2014–2015.

Figure 3 presents the spatial patterns of PM variables in the YRD via Ordinary Kriging Interpolation of ArcGIS. Simply, $PM_{2.5}$ concentrations in the north (particularly in the northwest) were apparently higher than in the south of the region. These patterns characterized by "increasing from the southeast to the northwest" were also observed for PM_{10} and the polluted-day number. In contrast, the $PM_{2.5}/PM_{10}$ ratio met the inverse varying trends. All these results revealed that severe PM pollution mainly occurred in the north, but $PM_{2.5}$ dominated the volume concentration in the south of the study region.

Relationship of daily $PM_{2.5}$ concentrations with RH

The seasonal difference of PM was greatly obvious based on the results of the previous section. Considering that temperature can differentiate the seasons to some degree, we used three variables, temperature, RH, and $PM_{2.5}$, to explore the complicated relationship between RH and the daily $PM_{2.5}$ concentrations. Let T and RH be the X and Y coordinates, respectively; the daily $PM_{2.5}$ distribution-related T and RH are illustrated in Fig. 4 via Surfer 10 and ArcGIS 10.2.

Interestingly, daily $PM_{2.5}$ concentrations were closely correlated with T and RH, shown in Fig. 4. High $PM_{2.5}$ concentrations exceeding 150 μg/m^3 not only frequently occurred in the condition with $T < 10$ °C and RH = 50–80% but also appeared in the condition

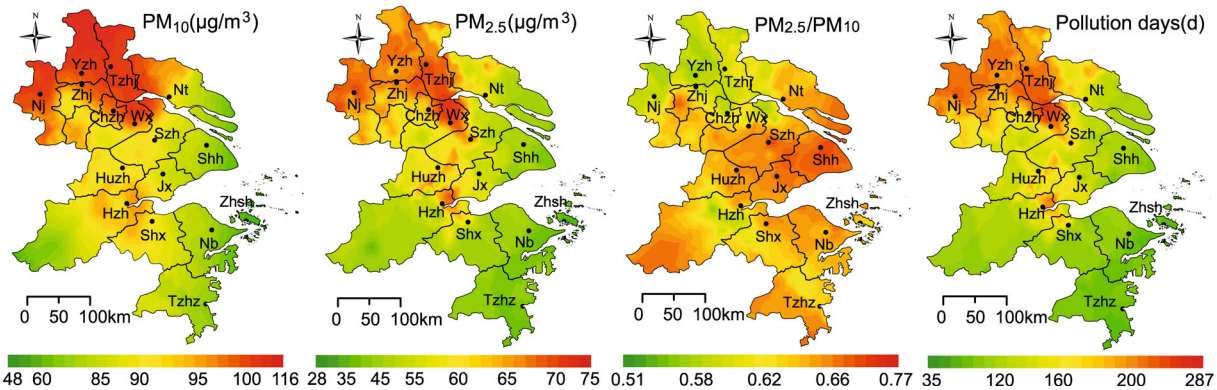

Fig. 3 Spatial distributions of the annual PM concentrations, the mean ratio of $PM_{2.5}/PM_{10}$, and the total polluted days in the YRD in 2014–2015

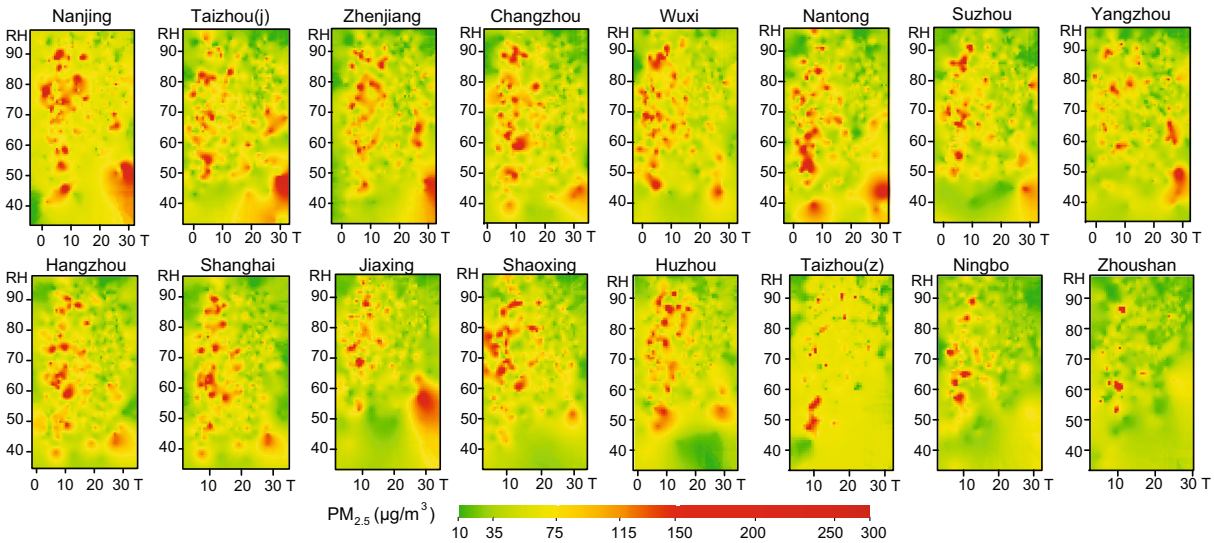

Fig. 4 $PM_{2.5}$ distribution related with RH and T (the values of RH (%), T (°C), and $PM_{2.5}$ (μg/m^3) used in this figure were all based on the daily average)

with $T > 30$ °C and RH < 50%. For instance, in Nanjing, 62% of 1673 pollution grids ($\rho(PM_{2.5}) \geq 75$ μg/m^3) were observed at RH = 60–80% and $T < 10$ °C, and 25% were located at RH < 60% and $T > 10$ °C. Additionally, in most cities, the number of pollution grids increased with RH growing when RH was between 50 and 80%, and then decreased at RH > 80%. In addition to that in winter, the conditions in summer accompanied with high T and low humidity also experienced serious $PM_{2.5}$ pollution, particularly in the heavily polluted cities (such as Nanjing, Taizhou(j), Zhenjiang). In general, these results indicate that $PM_{2.5}$ pollution is likely in two types of atmospheric environments, low-temperature and middle-range RH condition, or high-temperature and low RH condition, which was also suggested by Tran and Mölders (2011).

Statistical relationships between RH and PM pollution in the YRD region

Correlations of RH with $PM_{2.5}$ and PM_{10}

The equal step-size statistical method was used to further correlate RH to PM concentrations. It seems that RH was closely and regularly linked with PM (Fig. 5). Specifically, RH had an inverted V-shaped curve with PM_{10} concentrations (Fig. 5a–c) and an inverted U-shaped curve with $PM_{2.5}$ concentrations (Fig. 5d–f). With a rise in RH, PM_{10} significantly increased ($R = 0.63$, $P < 0.05$) for RH < 45%, followed by peaking at around RH = 45%, and then significantly decreased ($R = -0.96$, $P < 0.01$) for RH > 45%. Unlike the variations seen in PM_{10}, RH had an inverted U-shaped curve with $PM_{2.5}$ ($P < 0.01$, using two-factor analysis of variance). The curve of $PM_{2.5}$ could be specifically divided into three stages: stage 1 (an obvious increase ($R = 0.56$, $P < 0.05$) with sharp fluctuations at RH < 45%), stage 2 (steady fluctuation with a slight increase when RH = 45–70%), and stage 3 (a significant decrease ($R = -0.92$, $P < 0.01$) for RH > 70%). The variation patterns in 2014 and 2015 were similar to each other.

In short, the range of RH that caused $PM_{2.5}$ accumulation (RH < 70%) was larger than that impacting PM_{10} concentrations (RH < 45%), while the range of RH mitigating $PM_{2.5}$ concentrations (slope = − 0.94) was smaller than that for PM_{10} concentrations (slope = − 1.23).

For seasonality shown in Fig. 6, with RH increasing, PM_{10} had both increasing (RH < 45%) and decreasing trends (RH > 45%) in winter and in spring, but only had a decreasing stage during summer and autumn. These curves indicated that the accumulation effect of RH on PM_{10} was stronger in winter and spring, as compared with the effect in summer and autumn. The reduction effects were weakest in winter. For $PM_{2.5}$, the RH range that caused $PM_{2.5}$ increase was larger in winter (RH < 90%) and spring (RH < 80%), but smaller (RH < 70%) in summer and autumn. This denoted that the

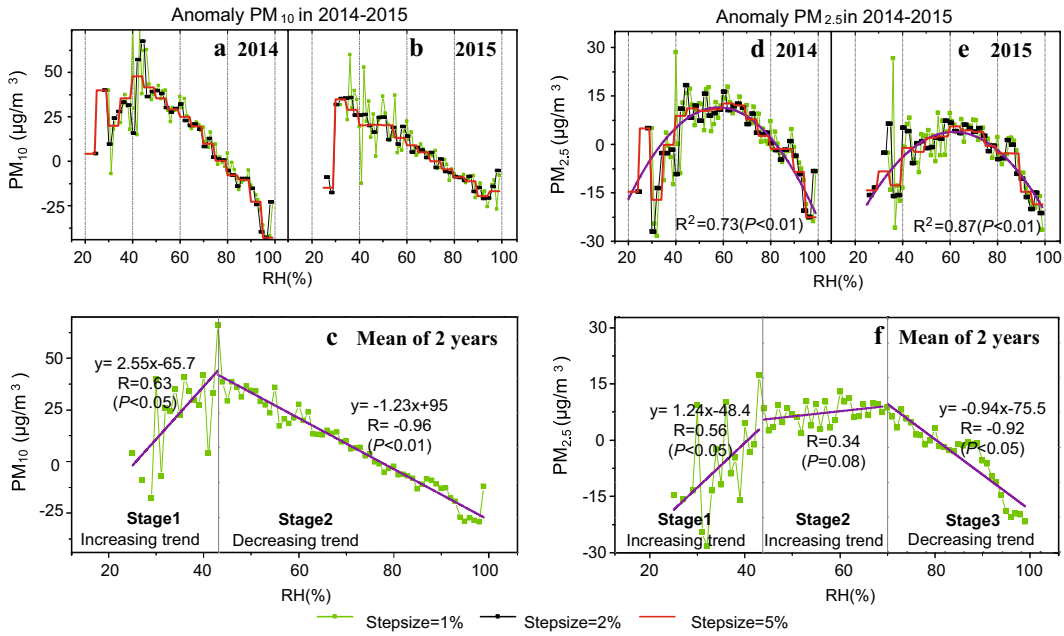

Fig. 5 Relationships of RH with PM_{10} and $PM_{2.5}$ concentration anomalies in 2014–2015

accumulation impact of RH was stronger at lower temperatures, tracking with the PM_{10}. In short, RH had a more intense accumulation effect on PM concentration in winter and spring, but a stronger reduction effect in summer and autumn.

Correlations between RH and the ratio of $PM_{2.5}/PM_{10}$

Figure 7 summarizes a response of the ratio of $PM_{2.5}/PM_{10}$ to RH in 2014–2015. No clear regularity in the ratio was observed at RH < 40%. However, at RH > 40%, the ratio trend became an upward line ($R = 0.96$, $P < 0.01$) with a slope of 0.004, which meant that a 1% increase in RH could bring a 0.004 increment in the ratio. The positive trend found further evidence that $PM_{2.5}$ was more dominant (by volume concentration) than PM_{10} as RH increased. Meanwhile, it revealed that the accumulation effect of RH on $PM_{2.5}$ was more intense than that on PM_{10}, and the reduction effects of RH on $PM_{2.5}$ was weaker than that on PM_{10}.

In four seasons, the curves were also characterized by a significant increase ($R > 0.91$, $P < 0.01$) for RH > 40%, and the slope in winter (0.006) was slightly larger than the slopes in the other three seasons (0.004–0.005). The

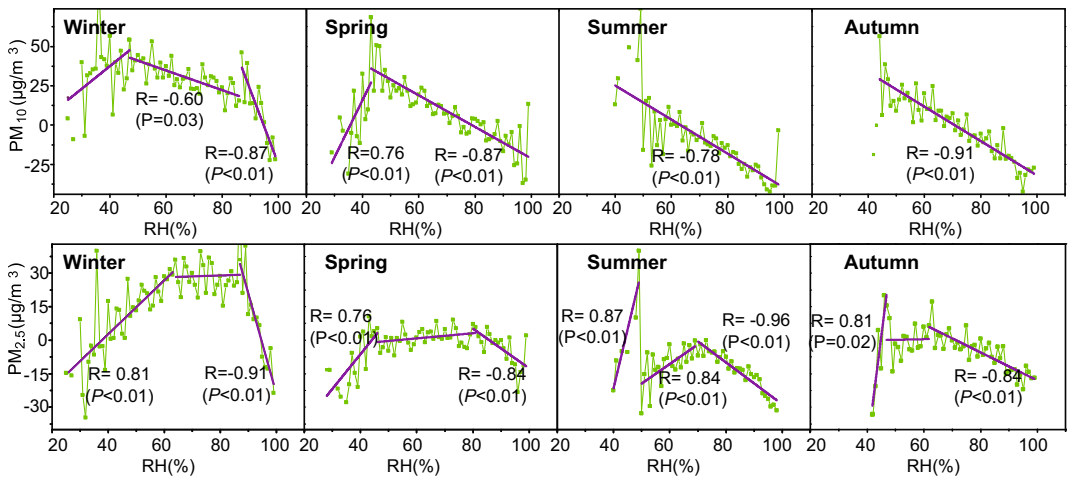

Fig. 6 Correlations of RH with anomaly in PM_{10} and $PM_{2.5}$ concentrations in each season (step-size = 1%)

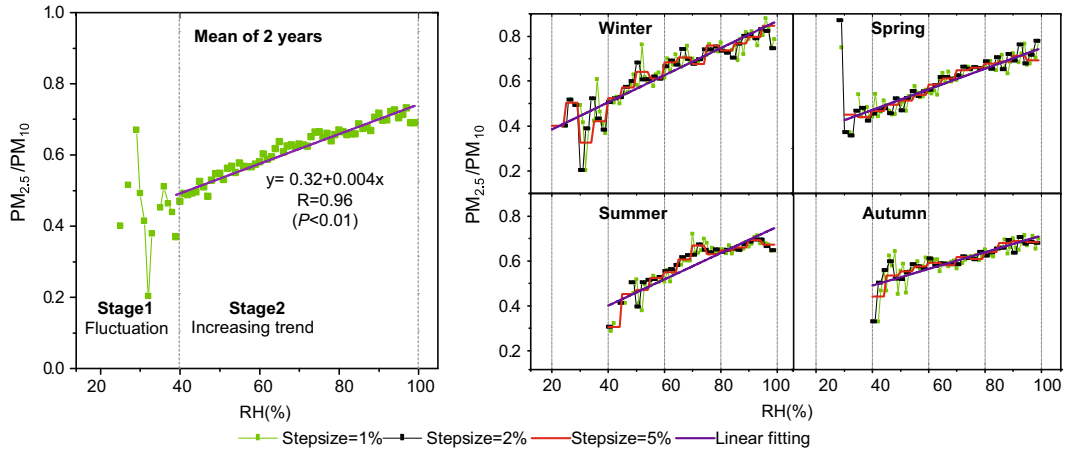

Fig. 7 Relationships between RH and $PM_{2.5}/PM_{10}$ ratio in 2 years (linear regression was conducted at the step-size of RH = 1%)

conclusions were in agreement with the results in Cheng et al. (2015).

Correlations between RH and polluted-day numbers

Due to the relatively sparse polluted-day numbers, we analyzed the associations between RH and pollution days at a step-size of RH = 5%. The inverted V-shaped curve in Fig. 8 indicated that the impact of humidity on the frequency of polluted days significantly changed on both sides of RH = 70%. A simple linear regression was used to fit the trend of the pollution days with RH increasing. Specifically, a 1% increase in RH could cause a 0.40 rise (R = 0.96, P < 0.01) in polluted-day numbers for RH = 40~70% and a 0.52 decrease (R = − 0.96, P < 0.01) in pollution days when RH > 70%. Regarding seasonality, the four seasons all have the inverted V-shaped curves, of which winter had the fastest growth in polluted-day numbers with RH rising.

Spatial variability in the relation between RH and PM pollution

Figure 9 illustrates the statistical relationships of RH with $PM_{2.5}$, PM_{10}, and polluted days in 16 cities. RH had a weak inverted V-shaped relationship (peaking at RH = 30–45%) with PM_{10}, a slightly inverted U-shaped relation (peaking at RH = 45–80%) with $PM_{2.5}$, and a significant inverted V-shaped relationship (peaking at RH = 65~75%) with the number of polluted days.

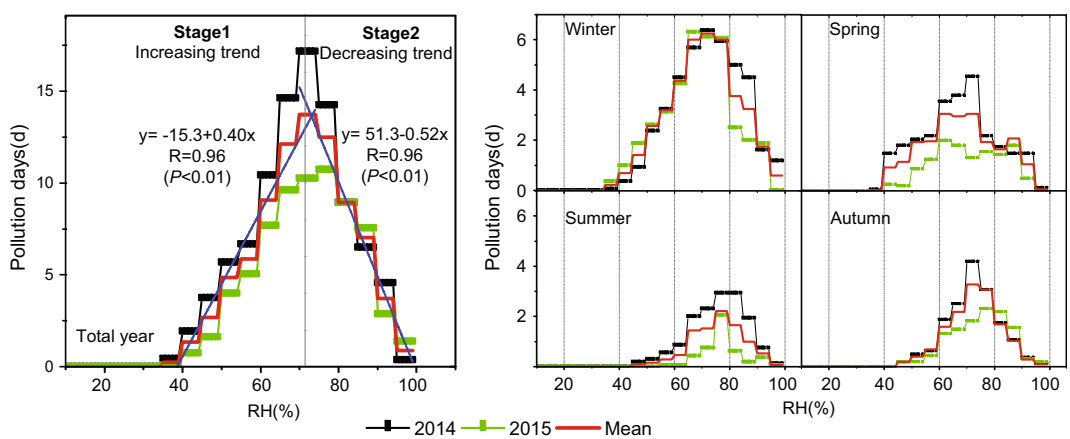

Fig. 8 The correlation between RH and pollution days in 2 years

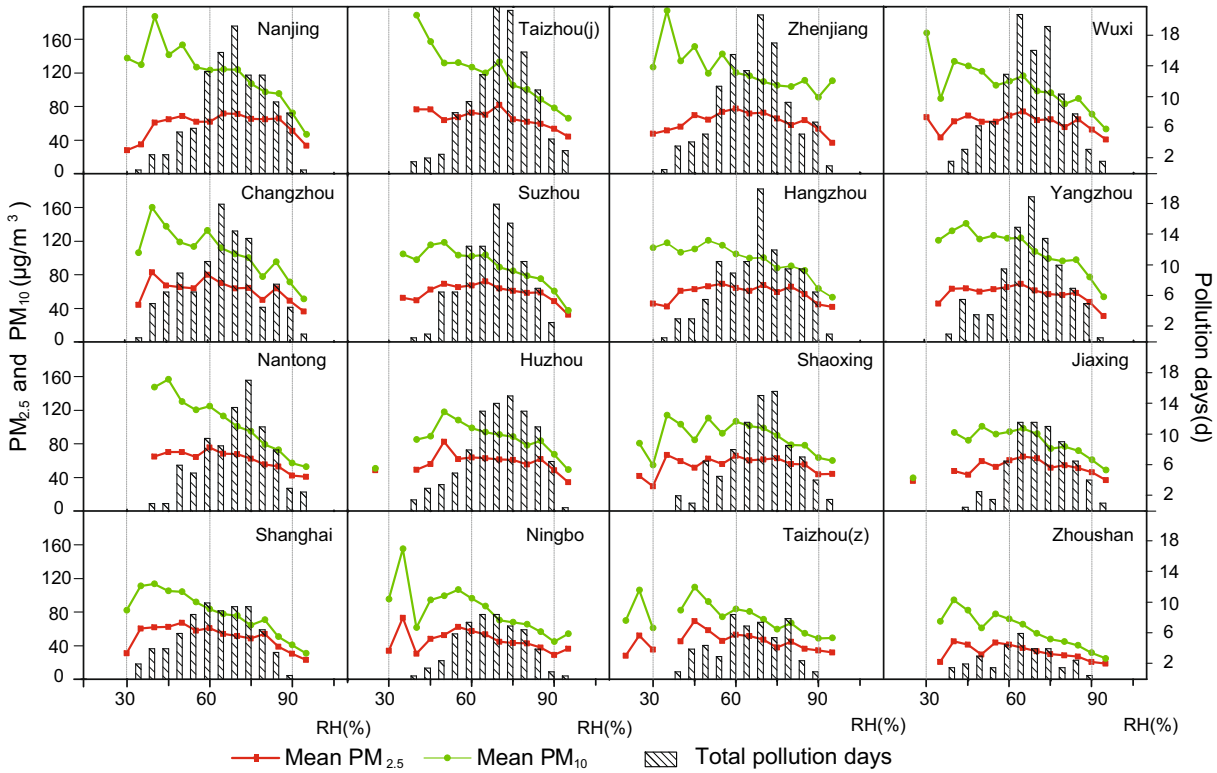

Fig. 9 Associations of RH with $PM_{2.5}$ and PM_{10} concentrations, and polluted days in 16 cities (with the step size of RH = 5%)

Figure 10 demonstrates the impacts of RH on PM as expressed by the slopes from linear regression models and their confidence levels. The positive slopes in Fig. 10a indicate that rising RH (at RH < 50%) could increase $PM_{2.5}$, and these accumulation impacts were significant in 50% out of the studied 16 cities, especially in the heavily polluted ones. For PM_{10} (Fig. 10b), we noted only two cities with a significant increasing trend ($P < 0.01$ or $P < 0.05$). However, the negative slopes in Fig. 10c, d reveal that the reduction effects of RH were significant not only on $PM_{2.5}$ (RH = 70–100%) but also on PM_{10} concentrations (RH = 45–100%).

RH types and their effects on PM pollution

Based on the varying patterns of $PM_{2.5}$ and PM_{10} concentrations at different RH levels, RH (0~100%) was

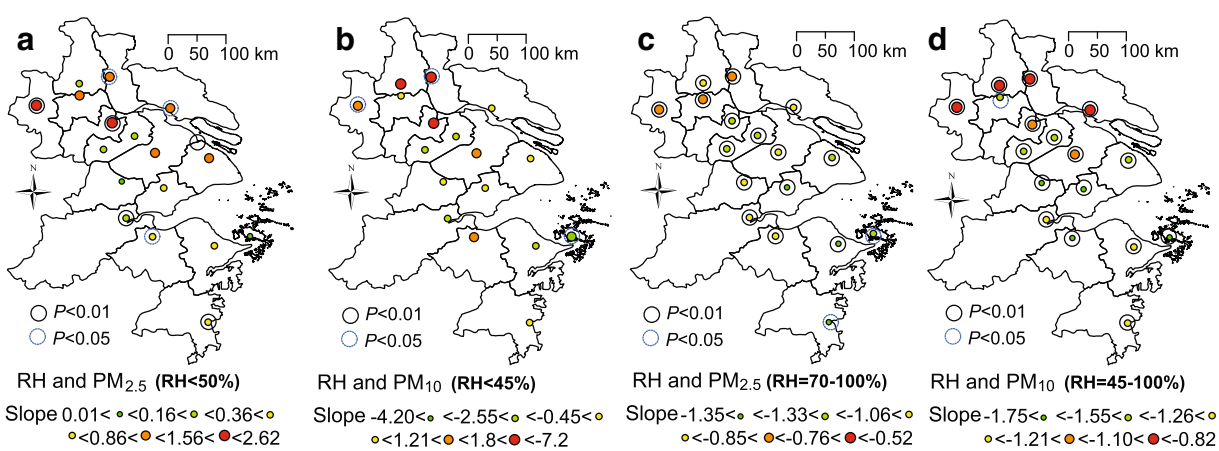

Fig. 10 Spatial patterns of the slope in linear regression and the confidence level

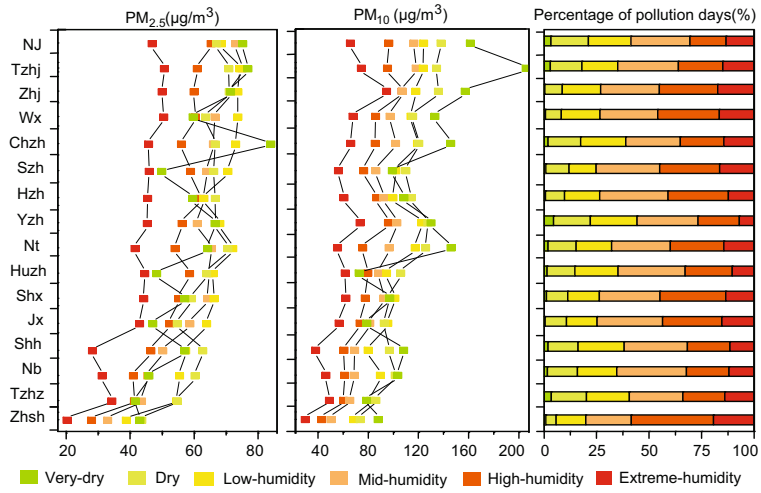

Fig. 11 $PM_{2.5}$ and PM_{10} concentrations and the percentage of pollution days of six RH regions in 16 cities

divided into six stages, < 45, 45–60, 60–70, 70–80, 80–90, and > 90%, which were defined as very-dry, dry, low-humidity, mid-humidity, high-humidity, and extreme-humidity conditions, respectively. Figure 11 describes the mean $PM_{2.5}$, the mean PM_{10}, and the percentage of pollution days in every RH stage. In specification, $PM_{2.5}$ averaged 62 ± 21, 57 ± 13, 56 ± 17, and 53 ± 21 μg/m^3, respectively, in very-dry, dry, low-humidity, and mid-humidity conditions (1.03–1.13 times of the annual concentration), but averaged 47 ± 18 and 35 ± 15 μg/m^3 in high-humidity and extreme-humidity conditions (only 0.93 and 0.73 times of the annual concentration), respectively. That is to say, the $PM_{2.5}$ accumulation stage at RH = 45–70% was an important contribution to the annual concentration. Similarly, the highest PM_{10} concentration was observed in a very-dry condition (139 ± 66 μg/m^3), followed by dry (105 ± 32 μg/m^3) and mid-humidity (96 ± 28 μg/m^3) conditions, and the lowest was in extreme-humidity condition (62 ± 32 μg/m^3). These data indicated the very-dry and dry conditions could cause PM accumulation, while the mid-humidity, high-humidity, and extreme-humidity conditions could remove particles and further mitigate air pollution.

To further investigate the spatial correlation of RH with PM pollution, the days situated every RH stage were counted out to correlate to the annual $PM_{2.5}$ and PM_{10} concentrations and total polluted days via Pearson correlation analysis (Table 2). Dry and high-humidity days played an important role in PM pollution in the YRD. Of them, dry days positively correlated with $PM_{2.5}$ (R = 0.632), PM_{10} (R = 0.646), and polluted-day numbers (R = 0.672), indicating that a higher number of dry days may cause more severe haze pollution. In contrast, high-humidity days had a negative significant correlation ($P < 0.01$) with PM pollution; thus, high RH can help mitigate PM pollution.

Based on the previous statistical results, we presented the effects of RH on PM in Fig. 12, as suggested by Jiang et al.(2016). Overall, increasing RH

TablFe 2 Correlations between the number of days in every RH ranges and PM variables

Types RH ranges		Annual $PM_{2.5}$	Annual PM_{10}	Total polluted days
Very-dry	< 45%	0.258	0.279	0.324
Dry	45–60%	0.632**	0.646**	0.672**
Low-humidity	60–70%	0.437	0.403	0.451
Mid-humidity	70–80%	0.355	0.275	0.257
High-humidity	80–90%	− 0.762**	− 0.745**	− 0.769**
Extreme-humidity	90–100%	− 0.252	− 0.19	− 0.221

*$P < 0.05$; **$P < 0.01$

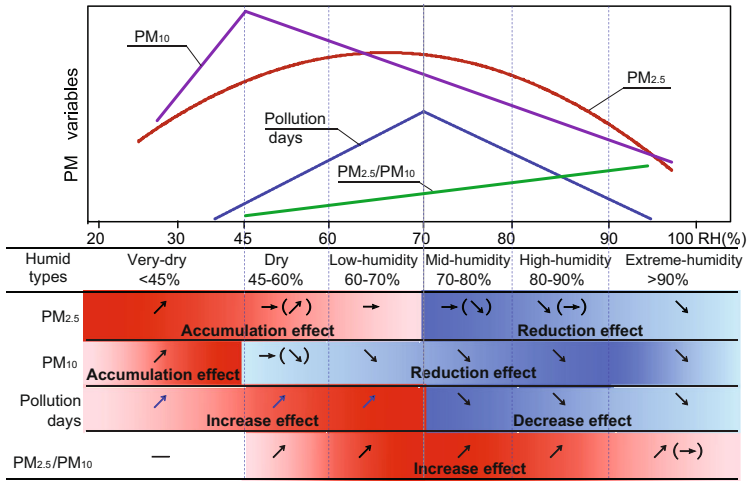

Fig. 12 Sketch of different RH-level effects on PM pollution (the arrows in this figure: ↗refers to an increasing trend; → refers to a stable trend; ↘ refers to a decreasing trend; →(↗) is a stable with slight increasing trend; →(↘) is a stable with slight decreasing trend; ↘(→) means a slow decreasing trend; and↗(→) means a slow increasing trend. In the same color, the deeper color represents the stronger influence)

created an accumulation effect on $PM_{2.5}$ at RH < 70% (including very-dry, dry, and low-humidity conditions), but had a reduction effect at RH > 70% (including the mid-humidity, high-humidity, and extreme-humidity conditions). For PM_{10}, an accumulation effect only occurred under the very-dry condition, while the reduction effects were found for the other RH ranges. Moreover, the increasing and decreasing effects of RH on the number of polluted days were comparable at RH = 70%. Unlike the abovementioned PM variables, the $PM_{2.5}/PM_{10}$ ratio increased continually with the rise in RH.

Discussion

Interpretation of the independent analysis of RH

A growing number of studies have examined the associations of RH with particle pollution, which is helpful for the government regarding the formulation of appropriate environmental policy. It is generally known that PM was greatly influenced by many natural factors besides RH. For instance, the temperature is one of the key factors impacting PM pollution. First, temperature influenced air stability considerably, playing an important role in particle accumulation or spreading. Second, when the air temperature rises during a $PM_{2.5}$ pollution episode, the active photochemical reactions highly favor the formation of sulfate, organic carbon, and elemental carbon and deter the condensation of nitrate. This causes an increase in the concentration of $PM_{2.5}$ and probably further aggravates haze pollution (Tai et al. 2010; Pateraki et al. 2012; Hua et al. 2015).

However, considering the space and aim of this paper, we only focused on the associations of RH with $PM_{2.5}$ and PM_{10} and the number of polluted days. The major reason for this exclusion was that RH seemed to be a combinational result of other meteorological conditions (e.g., T, WS, and precipitation). On the basis of statistics of RH in the 16 cities of the YRD, RH averaged 83 ± 6% on rainy days. More than 70% of rainy days had a high humidity environment with RH > 80%. This indicates that the high-humidity and extreme-humidity days were primarily affected by rainfall. Moreover, $PM_{2.5}$ pollution frequently occurred in stagnant conditions (with a lower WS and T, and a stable atmospheric environment) as suggested in previous studies (Tai et al. 2010; Wang et al. 2015). Approximately 70% of polluted days had a humidity condition with RH between 45 and 80%, showing that the dry, low-humidity, mid-humidity levels are the main characteristics of the stagnant conditions. Additionally, the days with RH < 45% accounted for 6% of total non-rainy days and accounted for 0.5% of rainy days, meaning that the very-dry condition frequently appeared in days without rainfall. For seasonality, the days with RH < 80% accounted for 73 ± 11% in winter and 69 ± 11% in spring, while the days with RH > 70% accounted for 85 ± 9% in summer and 72 ± 15% in autumn. The RH distributions indicated that the lower humidity was mostly observed in winter and spring, but higher humidity mainly appeared in summer and autumn. In this respect, RH also reflected the information of other weather conditions.

The mechanism of the impact from RH on PM

The present research regarding haze pollution suggested that PM_{10} originates primarily from construction activities, transportation, and soil dust. Because of its large diameter, PM_{10} is easily deposited through both dry and wet deposition processes (Langner et al. 2011; Witkowska and Lewandowska 2016). However, $PM_{2.5}$ is difficult to deposit only depending on its gravity (Sun et al. 2014). Therefore, the impacts of RH on $PM_{2.5}$ become more complicated than those on PM_{10}. Our conclusions also verified that the curves of $PM_{2.5}$ were more intricate than those of PM_{10}. Moreover, RH greatly influenced the secondary reactions (from precursors to particles), which played an important role in haze pollution in several studies (Liu et al. 2016a, b). To further analyze the complicated mechanism of RH impacting $PM_{2.5}$ in detail, we explore the effects of RH on SO_2 and NO_2 in the following sections.

Pursuant to similar curves of RH with SO_2 and NO_2 in Fig. 13, growing RH caused these air pollutants to increase at RH < 35, to peak at approximately RH = 35–50%, and then to rapid decrease at RH > 50%. For seasons, the accumulation and reduction stages were all significant in winter and spring, but only the reduction stage appeared in summer and autumn periods. Referring to Wang et al. (2014), most of the SO_2 and NO_2 had not converted to particles at RH < 35%, while the conversions almost completed at RH > 50%, indicating that secondary transformation mainly occurred at RH = 35–50%. These may explain our conclusions about why the high concentrations of SO_2 and NO_2 appeared at RH = 35%, and why the $PM_{2.5}$ concentrations increased significantly at RH < 50%. Additionally, the lower temperature did not favor the chemical conversion process, resulting in a greater accumulation of precursors in winter. In summer and autumn, gaseous pollutants had difficulty remaining in the air for a long time because of the unstable atmosphere and the increased gas-to-particle transformation rate driven by high temperature and RH (Tai et al. 2010; Hua et al. 2015).

Consequently, synthesizing the statistical results in this paper and the conclusions in previous articles, we divided the effects of RH on PM into five stages.

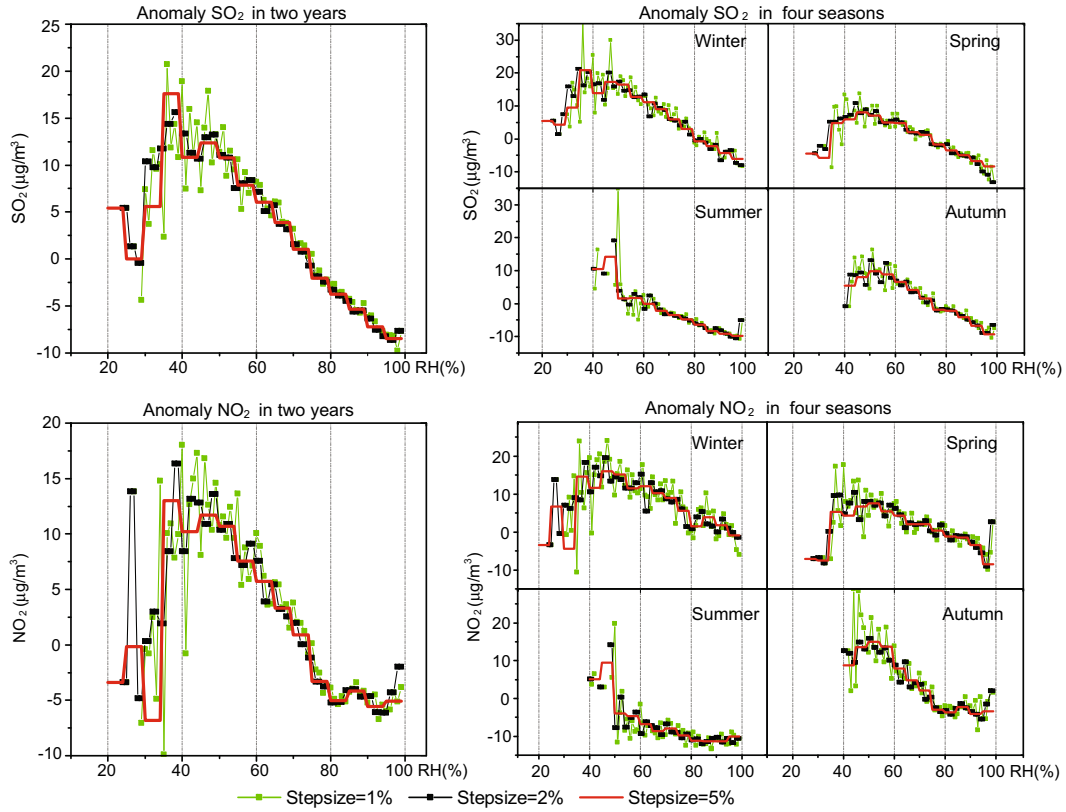

Fig. 13 Associations of RH with anomaly SO_2 and NO_2 concentrations

1. PM accumulation stage in very-dry condition (RH < 45%)—at this stage, anthropogenic emissions existed in the atmosphere mainly in the gaseous form or as primary particles. Due to the very low humidity, gravity deposition of fine particles was difficult, and the rate of secondary conversion was relatively slow. For this reason, PM_{10} concentrations were higher than $PM_{2.5}$ concentrations. However, since the very-dry condition was generally observed in low temperature and non-rainy days (causing PM accumulation), or was accompanied by high WS (which may bring additional PM from long-range transport), high PM concentration could also be observed in dry conditions. In total, the polluted days at this stage were very few.
2. PM accumulation and development stage in dry condition (RH = 45–60%)—growing RH accelerated the rates of conversion from SO_2 and NO_2 to SO_4^{2-} and NO_3^-, and of hygroscopic particle growth, all of which resulted in increases in the fine particle concentration (Hua et al. 2015). Simultaneously, the large-sized particles continued to grow through their hygroscopicity and began to experience gravity deposition. Therefore, at this stage, $PM_{2.5}$ concentrations increased and the number of pollution days began increasing, while PM_{10} concentrations began to decrease.
3. PM sustained growing stage in low-humidity condition (RH = 60–70%)—at this stage, most of SO_2 and NO_2 finished the conversion to SO_4^{2-} and NO_3^-, resulting in a stable increase in $PM_{2.5}$. PM_{10} continually decreased with humidity increasing. This stage was accompanied by a high $PM_{2.5}$ concentration and an explosive increase in the pollution-day numbers.
4. PM mitigation stage in mid-humidity condition (RH = 70–80%)—SO_2 and NO_2 concentrations were very low at this stage, and hence, the rate of secondary conversion also became slow. However, due to the sudden increase in deliquescence, the hygroscopicity of particles was enhanced by increasing RH (Wu et al. 2016). Although $PM_{2.5}$ and PM_{10} concentrations began to drop, $PM_{2.5}$ concentrations and the number of pollution days remained high.
5. PM removing stage in high-humidity and extreme-humidity conditions—at this stage, water in the air was close to saturation, which could enhance the condensation of water and the formation of rainfall, all of which in turn would reduce PM concentrations through scavenging, carrying, and gravity deposition. Meanwhile, at the onset of rainfall, the small rainfall amount and dust emissions caused by raindrops may increase the PM concentration to a certain extent. Thus, haze pollution was mitigated but would probably be accompanied with a small pollution peak in this stage.

Conclusion

This study examined the spatiotemporal characteristics of PM and its relationship with RH in the YRD. The chosen statistical method is effective and could verify the previous conclusions regarding the impact of RH on PM in recent articles. Our results clearly indicate that the PM was closely correlated with RH. In summary, the very-dry, dry, and low-humidity conditions (RH < 70%) positively influenced $PM_{2.5}$ and created accumulation effects, while the mid-humidity, high-humidity, and extreme-humidity conditions (RH = 70–100%) favored reducing $PM_{2.5}$ concentrations. Therefore, the trends of polluted days significantly change at RH = 70%. For PM_{10}, RH < 45% had an accumulation effect, but RH > 45% had a mitigation effect. Moreover, an increase in RH caused $PM_{2.5}$ to become increasingly preponderant in the ratio of particle volumes. Secondary transformation (from SO_2 and NO_2 to sulfate and nitrate) was the main reason for $PM_{2.5}$ pollution episodes. Thus, controlling precursors will be effective in reducing the fine particulate pollution, especially during winter in the YRD. This study could serve as a good reference for a future study on $PM_{2.5}$ mitigation. For instance, the effect of "fog-gun" dust-suppressing vehicles probably aggravate PM pollution in very-dry, dry, and low-humidity conditions. Our results may provide insight into the important impacts of RH on haze pollution and are helpful for optimizing an air-pollution control strategy.

Funding information This work was kindly supported by the National Natural Science Foundation of China (41401025, 31570459), the National Natural Science Youth Foundation of

Jiangsu Province of China (Grant BK20140921), and a Project Funded by the Priority Academic Program Development of Jiangsu Higher Education Institutions (PAPD).

References

Anda, A., Soos, G., Teixeira Da Silva, J. A., & Kozma-Bognar, V. (2015). Regional evapotranspiration from a wetland in Central Europe, in a 16-year period without human intervention. *Agricultural and Forest Meteorology, 205*, 60–72.

Catinon, M., Ayrault, S., Boudouma, O., Asta, J., Tissut, M., & Ravanel, P. (2012). Atmospheric element deposit on tree barks: the opposite effects of rain and transpiration. *Ecological Indicators, 14*(1), 170–177.

Cheng, Y., He, K., Du, Z., Zheng, M., Duan, F., & Ma, Y. (2015). Humidity plays an important role in the $PM_{2.5}$ pollution in Beijing. *Environmental Pollution, 197*, 68–75.

CMEP, 2016. National urban air-quality situation in 2015 released by the China National Environmental Monitoring Centre. http://www.zhb.gov.cn/gkml/hbb/qt/201602/t20160204_329886.htm, Accessed on 4 Feb 2016.

D'Angelo, L., Rovelli, G., Casati, M., Sangiorgi, G., Perrone, M. G., Bolzacchini, E., & Ferrero, L. (2016). Seasonal behavior of $PM_{2.5}$ deliquescence, crystallization, and hygroscopic growth in the Po Valley (Milan): implications for remote sensing applications. *Atmospheric Research, 176-177*, 87–95.

Du, H., Song, X., Jiang, H., Kan, Z., Wang, Z., & Cai, Y. (2016). Research on the cooling island effects of water body: A case study of Shanghai, China. *Ecological Indicators, 67*, 31–38.

Gao, M., Guttikunda, S. K., Carmichael, G. R., Wang, Y., Liu, Z., Stanier, C. O., Saide, P. E., & Yu, M. (2015). Health impacts and economic losses assessment of the 2013 severe haze event in Beijing area. *Science of the Total Environment, 511*, 553–561.

Han, L., Zhou, W., Li, W., & Li, L. (2014). Impact of urbanization level on urban air quality: a case of fine particles ($PM_{2.5}$) in Chinese cities. *Environmental Pollution, 194*, 163–170.

Hao, Y., & Liu, Y. (2016). The influential factors of urban $PM_{2.5}$ concentrations in China: a spatial econometric analysis. *Journal of Cleaner Production, 112*, 1443–1453.

Hasheminassab, S., Daher, N., Shafer, M. M., Schauer, J. J., Delfino, R. J., & Sioutas, C. (2014). Chemical characterization and source apportionment of indoor and outdoor fine particulate matter ($PM_{2.5}$) in retirement communities of the Los Angeles Basin. *Science of the Total Environment, 490*, 528–537.

Hsu, C., & Cheng, F. (2016). Classification of weather patterns to study the influence of meteorological characteristics on $PM_{2.5}$ concentrations in Yunlin County, Taiwan. *Atmospheric Environment, 144*, 397–408.

Hu, J., Wang, Y., Ying, Q., & Zhang, H. (2014). Spatial and temporal variability of $PM_{2.5}$ and PM_{10} over the North China Plain and the Yangtze River Delta, China. *Atmospheric Environment, 95*, 598–609.

Hua, Y., Cheng, Z., Wang, S., Jiang, J., Chen, D., Cai, S., Fu, X., Fu, Q., Chen, C., Xu, B., & Yu, J. (2015). Characteristics and source apportionment of $PM_{2.5}$ during a fall heavy haze episode in the Yangtze River Delta of China. *Atmospheric Environment, 123*, 380–391.

Huang, C., Chen, C. H., Li, L., Cheng, Z., Wang, H. L., Huang, H. Y., Streets, D. G., Wang, Y. J., Zhang, G. F., & Chen, Y. R. (2011). Emission inventory of anthropogenic air pollutants and VOC species in the Yangtze River Delta region, China. *Atmospheric Chemistry and Physics, 11*(9), 4105–4120.

Jiang, N., Scorgie, Y., Hart, M., Riley, M., Crawford, J., J. Beggs, P., Edwards, G., Chang, L., Salter, D., & Di Virgilio, G., (2016). Visualising the relationships between synoptic circulation type and air quality in Sydney, a subtropical coastal-basin environment: supporting information. International Journal of Climatology 37 (3), 1211–1228.

Kang, X., Cui, L., Zhao, X., Li, W., Zhang, M., Wei, Y., Lei, Y., & Ma, M. (2015). Effects of wetlands on reducing atmospheric fine particles $PM_{2.5}$ in Beijing. *Chinese Journal of Ecology, 34*(10), 2807–2813.

Kassomenos, P. A., Vardoulakis, S., Chaloulakou, A., Paschalidou, A. K., Grivas, G., Borge, R., & Lumbreras, J. (2014). Study of PM_{10} and $PM_{2.5}$ levels in three European cities: Analysis of intra and inter urban variations. *Atmospheric Environment, 87*, 153–163.

Langner, M., Kull, M., & Endlicher, W. R. (2011). Determination of PM_{10} deposition based on antimony flux to selected urban surfaces. *Environmental Pollution, 159*(8–9), 2028–2034.

Liu, Z., Hu, B., Zhang, J., Yu, Y., & Wang, Y. (2016a). Characteristics of aerosol size distributions and chemical compositions during wintertime pollution episodes in Beijing. *Atmospheric Research, 168*, 1–12.

Liu, J., Zhu, L., Wang, H., Yang, Y., Liu, J., Qiu, D., Ma, W., Zhang, Z., & Liu, J. (2016b). Dry deposition of particulate matter at an urban forest, wetland and lake surface in Beijing. *Atmospheric Environment, 125*, 178–187.

Masiol, M., Squizzato, S., Rampazzo, G., & Pavoni, B. (2014). Source apportionment of $PM_{2.5}$ at multiple sites in Venice (Italy): spatial variability and the role of weather. *Atmospheric Environment, 98*, 78–88.

Matsuda, K., Fujimura, Y., Hayashi, K., Takahashi, A., & Nakaya, K. (2010). Deposition velocity of $PM_{2.5}$ sulfate in the summer above a deciduous forest in central Japan. *Atmospheric Environment, 44*(36), 4582–4587.

Naeher, L. P., Holford, T. R., Beckett, W. S., Belanger, K., Triche, E. W., Bracken, M. B., & Leaderer, B. P. (1999). Healthy women's PEF variations with ambient summer concentrations of PM_{10}, $PM_{2.5}$, SO_4^{2-}, H^+, and O_3. *American Journal of Respiratory and Critical Care Medicine, 160*(1), 117–125.

Ouyang, W., Guo, B., Cai, G., Li, Q., Han, S., Liu, B., & Liu, X. (2015). The washing effect of precipitation on particulate matter and the pollution dynamics of rainwater in downtown Beijing. *Science of the Total Environment, 505*, 306–314.

Pateraki, S., Asimakopoulos, D. N., Flocas, H. A., Maggos, T., & Vasilakos, C. (2012). The role of meteorology on different sized aerosol fractions (PM_{10}, $PM_{2.5}$, $PM_{2.5\text{-}10}$). *Science of the Total Environment, 419*, 124–135.

Przybysz, A., Sæbø, A., Hanslin, H. M., & Gawroński, S. W. (2014). Accumulation of particulate matter and trace elements on vegetation as affected by pollution level, rainfall and the passage of time. *Science of the Total Environment, 481*, 360–369.

Pui, D. Y. H., Chen, S., & Zuo, Z. (2014). $PM_{2.5}$ in China: measurements, sources, visibility and health effects, and mitigation. *Particuology, 13*, 1–26.

Salameh, D., Detournay, A., Pey, J., Pérez, N., Liguori, F., Saraga, D., Bove, M. C., Brotto, P., Cassola, F., Massabò, D., Latella, A., Pillon, S., Formenton, G., Patti, S., Armengaud, A., Piga, D., Jaffrezo, J. L., Bartzis, J., Tolis, E., Prati, P., Querol, X., Wortham, H., & Marchand, N. (2015). $PM_{2.5}$ chemical composition in five European Mediterranean cities: a 1-year study. *Atmospheric Research, 155*, 102–117.

Stone, E., Schauer, J., Quraishi, T. A., & Mahmood, A. (2010). Chemical characterization and source apportionment of fine and coarse particulate matter in Lahore, Pakistan. *Atmospheric Environment, 44*(8), 1062–1070.

Sun, R., Chen, A., Chen, L., & Lü, Y. (2012). Cooling effects of wetlands in an urban region: the case of Beijing. *Ecological Indicators, 20*, 57–64.

Sun, F., Yin, Z., Lun, X., Zhao, Y., Li, R., Shi, F., & Yu, X. (2014). Deposition velocity of $PM_{2.5}$ in the winter and spring above deciduous and coniferous forests in Beijing, China. *PLoS One, 9*(5), 1–11.

Tai, A. P. K., Mickley, L. J., & Jacob, D. J. (2010). Correlations between fine particulate matter ($PM_{2.5}$) and meteorological variables in the United States: implications for the sensitivity of $PM_{2.5}$ to climate change. *Atmospheric Environment, 44*(32), 3976–3984.

Tallis, M., Taylor, G., Sinnett, D., & Freer-Smith, P. (2011). Estimating the removal of atmospheric particulate pollution by the urban tree canopy of London, under current and future environments. *Landscape and Urban Planning, 103*(2), 129–138.

Tian, G., Jiang, J., Yang, Z., & Zhang, Y. (2011). The urban growth, size distribution and spatio-temporal dynamic pattern of the Yangtze River Delta megalopolitan region, China. *Ecological Modelling, 222*(3), 865–878.

Tran, H. N. Q., & Mölders, N. (2011). Investigations on meteorological conditions for elevated $PM_{2.5}$ in Fairbanks, Alaska. *Atmospheric Research, 99*(1), 39–49.

Wang, J., & Ogawa, S. (2015). Effects of meteorological conditions on $PM_{2.5}$ concentrations in Nagasaki, Japan. *International Journal of Environmental Research and Public Health, 12*(8), 9089–9101.

Wang, W., Gong, D., Zhou, Z., & Guo, Y. (2012). Robustness of the aerosol weekly cycle over Southeastern China. *Atmospheric Environment, 61*, 409–418.

Wang, Y., Yao, L., Wang, L., Liu, Z., Ji, D., & Tang, G. (2014). Mechanism for the formation of the January 2013 heavy haze pollution episode over central and eastern China. *Science China: Earth. Sciences, 44*(1), 15–26.

Wang, P., Cao, J., Tie, X., Wang, G., Li, G., Hu, T., Wu, Y., Yunsheng Xu, G. X. Y. Z., & Zhan, C. (2015). Impact of meteorological parameters and gaseous pollutants on $PM_{2.5}$ and PM_{10} mass concentrations during 2010 in Xi'an, China. *Aerosol and Air Quality Research, 15*, 1844–1854.

Witkowska, A., & Lewandowska, A. U. (2016). Water soluble organic carbon in aerosols (PM_1, $PM_{2.5}$, PM_{10}) and various precipitation forms (rain, snow, mixed) over the southern Baltic Sea station. *Science of the Total Environment, 573*, 337–346.

Wu, D., Cao, S., Tang, L., Xia, J., Lu, J., Liu, G., Yang, M., Li, F., & Gai, X. (2016). Variation of size distribution and the influencing factors of aerosol in northern suburbs of Nanjing. *Environmental Science, 37*(9), 3269–3279.

Xu, J., Yan, F., Xie, Y., Wang, F., Wu, J., & Fu, Q. (2015). Impact of meteorological conditions on a nine-day particulate matter pollution event observed in December 2013, Shanghai, China. *Particuology, 20*, 69–79.

Zhu, L., Liu, J., Cong, L., Ma, W., Ma, W., & Zhang, Z. (2016). Spatiotemporal characteristics of particulate matter and dry deposition flux in the Cuihu wetland of Beijing. *PLoS One, 11*(7), e0158616. https://doi.org/10.1371/journal.pone.0158616.